Cancer Chemotherapy and Pharmacology (2022) 89:217–229
https://doi.org/10.1007/s00280-021-04392-1

ORIGINAL ARTICLE

Extracellular vesicles carry miR-27a-3p to promote drug resistance of glioblastoma to temozolomide by targeting BTG2

Lei Chen[1,2] · Zhangke Li[1,2] · Shuaibing Hu[2] · Qiqi Deng[2] · Puheng Hao[2] · Shiwen Guo[1]

Received: 21 July 2021 / Accepted: 21 December 2021 / Published online: 17 January 2022

Abstract

Objective Glioblastoma (GBM) is the most common central nervous system tumor. Temozolomide (TMZ) is a commonly used drug for GBM management. This study explored the mechanism of extracellular vesicles (EVs) regulating TMZ-resistance in GBM.

Methods LN229 cells were inducted into TMZ-resistant LN229r strain by stepwise induction. After the intervention of miR-27a-3p expression, cell viability of GBM cells treated with different concentrations of TMZ was detected by MTT and IC50 value was calculated. Cell proliferation and apoptosis were detected by colony formation and flow cytometry. EVs extracted from LN18 cells were identified and the internalization of EVs by LN229r cells was evaluated. The 100 μmol/L TMZ-treated LN229r cells were treated with EVs or EVs with downregulated miR-27a-3p to verify the effect of EVs-carried miR-27a-3p on TMZ resistance. The binding relation between BTG2 and miR-27a-3p was verified. miR-27a-3p and BTG2 expressions in GBM cells and EVs were detected by RT-qPCR. The BTG2 effect on TMZ-resistance in GBM was verified. The xenograft tumor nude mouse model was established by injecting LN229r cells and treated with EVs and 100 μmol/L TMZ.

Results miR-27a-3p was highly expressed in LN229r cells. IC50 value and proliferation of LN229r cells with silenced miR-27a-3p were decreased and apoptosis was increased, indicating that miR-27a-3p silencing reduced the drug-resistant cell LN229r resistance to TMZ. LN18-derived EVs could be internalized by LN229r cells, and release its encapsulated miR-27a-3p into LN229r cells and increase miR-27a-3p expression. EV treatment increased LN229r cell proliferation and reduced apoptosis, while EVs with silenced miR-27a-3p showed the opposite trend. miR-27a-3p targeted BTG2. BTG2 overexpression reduced LN229r cell resistance to TMZ. In vivo, after EVs treatment, tumor volume and weight, Ki67-positive rate, and miR-27a-3p were increased, while BTG2 expression was decreased.

Conclusion GBM-derived EVs were internalized by GBM cells, released miR-27a-3p into GBM cells, upregulated miR-27a-3p expression, and targeted BTG2, thus promoting TMZ resistance.

Keywords Glioblastoma · Extracellular vesicles · Temozolomide · miR-27a-3p · Drug resistance · BTG2 · Xenograft tumor

Introduction

Glioblastoma (GBM) is a common primary tumor of the spinal cord and brain, which histologically shares the characteristics of normal glial cells [1]. Although GBM is relatively rare, it's the most aggressive form of malignant primary tumor of the brain and leads to significant morbidity and mortality worldwide with a poor prognosis of only about 28.4% of the patients surviving 1 year and 3.4% surviving 5 years [2, 3]. Besides the influence of age, a variety of demographical aspects and stress, such as chemical exposure and alcohol consumption affect the incidence and manifestation of GBM [4]. Temozolomide (TMZ) is an alkylating agent, which has shown an anti-tumor effect as

Lei Chen and Zhangke Li are co-first authors.

✉ Shiwen Guo
Guoshiwen1120@163.com

[1] Department of Neurosurgery, The First Affiliated Hospital of Xi'an Jiaotong University, No. 277 Yanta West Road, Xi'an 710061, Shaanxi, People's Republic of China

[2] Department of Neurosurgery, Xi'an International Medical Center Hospital, Xi'an 710100, Shaanxi, People's Republic of China

a single agent in GBM treatment [5]. At present, although there are intensive researches and therapeutic options for GBM, including chemotherapy with TMZ, radiotherapy, and surgery, the prognosis of the patients with GBM is very poor due to notorious drug resistance [4, 6]. Further investigations are needed on the drug resistance in GBM.

Extracellular vesicles (EVs) are the bilayer-enclosed structures with a diameter of 30–1000 nm, which are important mediators for the intercellular communication of tumor cells and other cells that are also located in the microenvironment but in the sites far away by transferring nucleic acids and proteins (lncRNA, miRNA, mRNA) [3, 7]. microRNAs (miRNAs) are a variety of noncoding single-stranded RNAs with 18–22 nucleotides that post-transcriptionally influence the expression of genes through binding to the regions of 3'-UTR in the mRNAs and various specific miRNAs are deregulated in GBM, which are involved in the drug-resistant regulation [8]. EVs affect drug resistance in the tumor microenvironment through carrying miRNAs [9]. miRNAs are reported to play a role in modulating the TMZ-resistance of the GBM cells [10]. miR-27a-3p is involved in radiotherapy-resistance in GBM [11]. However, whether EVs can carry miR-27a-3p into GBM cells and thus play a role in TMZ-resistance of GBM is largely unknown. The downstream targets of miR-27a-3p were predicted using the database. B-cell translocation gene 2 (BTG2) was obtained. BTG2 is identified to be an anti-proliferation gene with the protein product of it affecting various cellular processes, such as messenger RNA stability, DNA repair, cell division, and transcriptional regulation, which is often downregulated in tumors and its reduction is related to the cell malignant behavior and poor outcome of the patients with cancers [12]. BTG2 is reported to be downregulated in human GBM tissues and is significantly related to a worse prognosis [13]. However, there is no domestic and foreign report at present on the effect and mechanism of EVs shuttled miR-27a-3p on the TMZ-resistance of GBM. This study investigated the mechanism of EVs derived miR-27a-3p on the TMZ resistance of GBM, so as to provide a theoretical basis for GBM treatment.

Materials and methods

Ethics statement

All procedures were authorized by the academic ethics committee of The First Affiliated Hospital of Xi'an Jiaotong University. The experiment was carried out in strict accordance with the guidelines for the management and use of laboratory animals issued by the Laboratory Association of China.

Cell culture

Human GBM cell lines LN18, LN229, and T98G (ATCC, Manassas, VA, USA) were cultured using ATCC's recommendations to 80% confluence in 75 cm^2 flasks in complete Dulbecco's modified Eagle's medium (DMEM, Thermo Fisher Scientific Inc., Waltham, MA, USA) containing 5% fetal bovine serum (FBS, Thermo Fisher Scientific Inc.) at 37 ℃/5% CO_2. According to the published literature [14], LN18 and T98G cells were selected as chemoresistant strains and LN229 as chemosensitive strains.

Stepwise induction of drug-resistant strains

LN229 cells were seeded into a 25 cm^2 culture flask at 1×10^5/mL. After 24 h cell adhesion, the cells were cultured in complete medium with the initial induction concentration of 10 μg/mL TMZ until the cell confluence reached 80–90%, and then cells were subcultured. The cells were seeded at a proper proportion into a new culture flask. After the cell adhesion was stable, the medium was refreshed with a fresh medium containing 10 μg/mL TMZ for further induction. The concentration of TMZ was doubled after repeated induction 5 times. When the induced concentration of TMZ reached 100 μg/mL, the increase of the concentration was stopped and the concentration was maintained. Each induction concentration was maintained for 20–30 d and LN229 resistant strains LN229r was successfully constructed after 6 months. The drug resistance was maintained using TMZ at a final concentration.

Lentivirus transfection

The lentivirus carrying miR-27a-3 was packaged according to the operation manual of GenePharma (Shanghai, China). In short, LN18 cells were infected by the lentivirus carrying miR-27a-3p in 5 μg/mL polybrene. After the infection for 72 h, LN18 cells were treated with puromycin dihydrochloride (Thermo Fisher Scientific Inc.) for 2 weeks and the cells stably expressing miR-27a-3p were obtained.

Extraction and identification of EVs

When the confluence of LN18 cells or LN18 cells with downregulated expression of miR-27a-3p was 70%, the medium was discarded. The sample was washed twice with phosphate-buffered saline (PBS) and the medium was refreshed with the medium made of EVs-free FBS (FBS was centrifuged at 100,000 g for 18 h to remove EVs). The supernatant was collected after continuous culture for 48 h and centrifuged at different speeds. The steps were as follows:

at 300 g for 10 min, at 1000 g for 20 min, at 10,000 g for 30 min, at 100,000 g at 4 ℃ for 3 h after filtration with 0.22 μm filter (Millex-GP, EMD Millipore, Darmstadt, Germany). The supernatant was removed and the precipitation obtained was resuspended with PBS. The sample was centrifuged at 100,000 g at 4 ℃ for 3 h and the supernatant was removed. The precipitate obtained at this time was the EVs (EVs, EVs-NC, EVs-inhibitor). The sample was resuspended with PBS. The protein quantification of EVs was determined using the bicinchoninic acid (BCA) protein quantitative kit (Beyotime, Shanghai, China). The morphology and the size distribution of EVs were observed using transmission electron microscopy (TEM, Hitachi, Japan) and nanoparticle tracking analysis (NTA, Malvern Instruments Ltd., Malvern, UK) [15]. Western blot (WB) was used to analyze the expressions of surface antigens CD63, CD9, and calnexin. In addition, GW4869 (living cell EVs inhibitor, 20 μg/mL, Sigma-Aldrich, St. Louis, MO, USA) was added into LN18 cells following the instructions. The precipitates extracted using the above method were resuspended in PBS and used as the GW group. The EVs were added with RNase I (Thermo Fisher Scientific Inc.) and heat-inactivated and used as RNase group.

Dil-labeled EVs

After NTA quantification, the extracted EVs were diluted with PBS and adjusted to the same number of particles and mixed evenly with Dil dyeing solution (RiboBio, Guangzhou, China) according to the volume ratio of 500:1. The sample was incubated at 37 ℃ in the dark for 15 min. After the incubation, the sample was centrifuged at 16,000 g for 60 min and the supernatant was removed. The sample was washed with PBS 3 times to remove the excess dye. The labeled EVs were co-cultured with LN229r cells. After 48 h, the sample was washed with PBS 3 times, added with immunostaining fixative (Beyotime), and then placed for 15 min at room temperature, added with 4',6-diamidino-2-phenylindole (DAPI, Solarbio, Beijing, China) and 0.5 mL anti-fluorescence quenching sealing solution (Beyotime), observed and imaged under the fluorescence microscope (Olympus Optical Co., Ltd, Tokyo, Japan).

Cell grouping

miR-27a-3p mimic and the NC, pcDNA-NC, and pcDNA-BTG2 were purchased from GenePharma company. miR-27a-3p mimic and the NC (50 nM) were transfected into LN229 cells, and pcDNA-NC and pcDNA-BTG2 (40 nM) were transfected into LN229r cells using Lipofectamine 2000 (Thermo Fisher Scientific Inc.). LN229r cells were infected with lentivirus of silencing miR-27a-3p or its NC (GenePharma, 5 μg/mL). LN229r cells were treated with LN18-conditioned medium after treatment of 30 μg EVs, EVs-NC, EVs-inhibitor, or GW4869. The following experiment was carried out 24 h later.

Colony formation assay

The cell proliferation and effects of gene manipulation and/or drug therapy were evaluated by colony formation assay. Briefly, the cells (500 cells/well) were seeded into a 6-well plate. The colonies were fixed with methanol and stained with 0.1% crystal violet on the 10th day. The colony was microscopically observed under a light microscope. Each of the dishes containing ≥ 50 cell colonies was counted and imaged using a digital camera (Olympus Optical Co., Ltd).

3-(4,5-dimethylthiazol-2-yl)-2,5-diphenyltetrazolium bromide (MTT) assay

Cells in the logarithmic phase were collected and treated with different concentrations of TMZ (0, 25, 50, 100, 200, and 400 μmol/L). The concentration of cell suspension was adjusted to 1×10^5/mL, and the cells were seeded into 96-well plates at 100 μL/well, incubated in 5% CO_2 incubator at 37 ℃ for 48 h, and observed under an inverted microscope (Leica, Wetzlar, Germany). Each well was added with 10 μL MTT solution (Sigma, 5 mg/mL, 0.5%MTT) and the cells were cultured for 4 h. The cells were centrifuged (400 g, 15 min) carefully and the supernatant was washed off. Each well was added with 200 μL dimethyl sulfoxide (DMSO) and the sample was shaken in a decolorizing shaker for 20 min to fully dissolve the crystal. The optical density (OD) value of each well was detected at 570 nm using a microplate reader (Bio-Rad, Hercules, CA, USA).

Flow cytometry

The cells to be detected were detached and centrifuged and resuspended with PBS. The cells were counted and the suspension was adjusted to 100 cells/μL. Then, 1 mL suspension was drawn into the centrifuge tube and centrifuged at 250 g for 5 min. The supernatant was removed. The cell precipitate was resuspended using 200 μL Annexin V-fluorescein isothiocyanate (FITC) binding solution. The sample was incubated in the dark for 10 min. The sample was centrifuged at 250 g for 5 min after the incubation and the supernatant was removed. The sample was added with 190 μL Annexin V-FITC binding solution and 10 μL propidium iodide (PI) staining solution, evenly mixed, incubated in the dark for 10 min, and detected using flow cytometry (Beckman Coulter, Brea, CA, USA).

Dual-luciferase assay

The wild type (WT) and mutant type (MUT) vectors (Ambion, Austin, TX, USA) of BTG2 were constructed following the binding sites predicted using TargetScan database (http://www.targetscan.org/vert_71/) [16]. The vectors were cotransfected with mimic NC or miR-27a-3p mimic into the 293 T cells using the Lipofectamine 2000. The activity of relative luciferase was detected using Dual-Lucy Assay Kit (Solarbio, Beijing, China). After 48 h of transfection, the cells were collected and detected using the dual-luciferase reporter gene detection system (Promega, Madison, WI, USA).

Western blot

The protein of EVs was extracted using RIPA lysate and the extracted protein was determined using BCA (Beyotime). The 30 μg protein was isolated by 10% SDS-PAGE and transferred to polyvinylidene fluoride membranes, which were blocked with 5% bovine serum albumin at room temperature for 1 h, and added with the corresponding primary antibodies CD9 (1:2000, ab92726, Abcam, Cambridge, MA, USA), CD63 (1:1000, ab134045, Abcam), calnexin (1:1000, ab133615, Abcam) and actin (1:1000, ab8227, Abcam) at 4 ℃ overnight. Next, the membranes were added with secondary antibody (1:2000, ab205718, Abcam) for 1 h. The enhanced chemiluminescence was used for development and Image J software (NIH, Bethesda, MD, USA) was used to quantify the gray scale.

Xenograft tumor model in nude mice

BALB/c female athymic nude mice (6 weeks old, weighing 18-22 g) used for GBM xenograft model establishment were purchased from Beijing Vital River Laboratory Animal Technology Co., Ltd [SYXK (Beijing) 2017-0033, Beijing, China]. The mice were raised in a micro-isolation cage. The nude mice were injected with 5×10^5 LN229r cells through the right abdomen. About 3 weeks later, when the measurable tumor could be touched (about 100 mm^3), the mouse was treated with 100 μmol/L. The nude mice were assigned into 4 groups ($N = 12$ in each group): LN229r group (injected with LN229r); LN229r + TMZ group (injected with LN229r + TMZ); LN229r + GW + TMZ group (injected with LN229r + GW4869 treated LN18-conditioned medium and TMZ); LN229r + EVs + TMZ group (injected with LN229r + 30 μg EVs + TMZ). The injections were performed 5 times a week. The mice were monitored every day and the tumor size was measured every 7 day. The tumor volume formula was: tumor volume $(mm^3) = (\text{width}) \times (\text{height})^2/2$. On the 28th day of injection, the nude mice were euthanized by intraperitoneal injection of ≥ 100 mg/kg pentobarbital sodium. After tumor dissecting and weight measurement, 6 nude mice of each group were used for immunohistochemistry and the other 6 for reverse transcription quantitative polymerase chain reaction (RT-qPCR).

Immunohistochemistry

The tumor tissue was embedded with paraffin and cut into 5 μm-thick sections, dewaxed, dehydrated, and repaired in antigen repair solution, and then blocked at room temperature with goat serum (Beyotime) for 20 min and then goat serum was removed. The sections were incubated with Ki67 primary antibody (ab16667, Abcam) at 4 ℃ overnight, incubated with a corresponding secondary antibody (ab205718, Abcam) for 1 h at room temperature, and further detected using diaminobutyric acid (DAB) system (Beyotime).

RT-qPCR

The TRIzol (Invitrogen, Carlsbad, CA, USA) was used to extract the total RNA of cells or tumor tissue. The concentration and purity of RNA were detected using NanoDrop 2000. Following the instructions of the SYBR Premix Ex Tap™ II kit (Takara, Shiga, Japan), fluorescent quantitative PCR was performed on ABI 7500 quantitative PCR instrument (7500, ABI, Foster City, CA, USA). GAPDH and U6 were internal parameters and the $2^{-\Delta\Delta Ct}$ method [17] was used to calculate. The primer sequences are shown in Table 1.

Statistical analysis

All data were processed by SPSS21.0 statistical software (IBM Corp. Armonk, NY, USA). Normal distribution and homogeneity of variance tests were performed and the values were in normal distribution and the variance was homogeneous. The data were described as mean ± standard deviation.

Table 1 Primer sequence

Gene	Forward 5'-3'	Reverse 5'-3'
miR-27a-3p	TTCACAGTGGCTAAGTTCCGC	GCGGAACTTAGCCACTGTGAA
BTG2	ATGAGCCACGGGAAGGGAACCGAC	CTAGCTGGAGACTGCCATCACGTA
GAPDH	ATGGTTTACATGTTCCAATATG	TTACTCCTTGGAGGCCATGTGG
U6	CGCTTCGGCAGCACATATAC	AATATGGAACGCTTCACGA

Independent *t* test was applied for the comparison between two groups and one-way analysis of variance (ANOVA) was applied for the comparison among multi groups. Tukey's multiple comparisons test was used for the post hoc test. $P < 0.05$ indicated statistical significance.

Results

miR-27a-3p was highly expressed in TMZ-resistant GBM cells

miR-27a-3p can induce TMZ resistance in GBM [18], but its specific mechanism needs further study. To investigate the role of miR-27a-3p in the TMZ resistance of GBM, we firstly induced LN299 cell line into TMZ resistant cell line step by step. Colony formation assay showed that after TMZ treatment, the number of colonies in the LN229r group was higher than that in the LN229 group, indicating the successful induction ($P < 0.01$, Fig. 1A). In addition, the IC50 of GBM cells was verified using the MTT method. The results showed that the IC50 of LN229r (resistant) was 152.65 μg/mL, which was much higher than that of LN18 (resistant), T98G (resistant) and LN229 (sensitive) (LN18: 86.54 μg/mL; T98G: 98.59 μg/mL; LN229: 20.14 μg/mL) ($P < 0.01$, Fig. 1B). These results indicated that we successfully constructed a TMZ-resistant strain LN229r. Subsequently, the expression of miR-27a-3p in GBM cells was detected by RT-qPCR and it was found that miR-27a-3p was highly expressed in TMZ-resistant cells ($P < 0.01$, Fig. 1C). In addition, the relation between miR-27a-3p expression and the survival of GBM patients was predicted using ENCORI Pan-Cancer Analysis Platform database (http://starbase.sysu.edu.cn/panCancer.php) and it was found that the prognosis of patients with high miR-27a-3p expression was worse ($P < 0.01$, Fig. 1D).

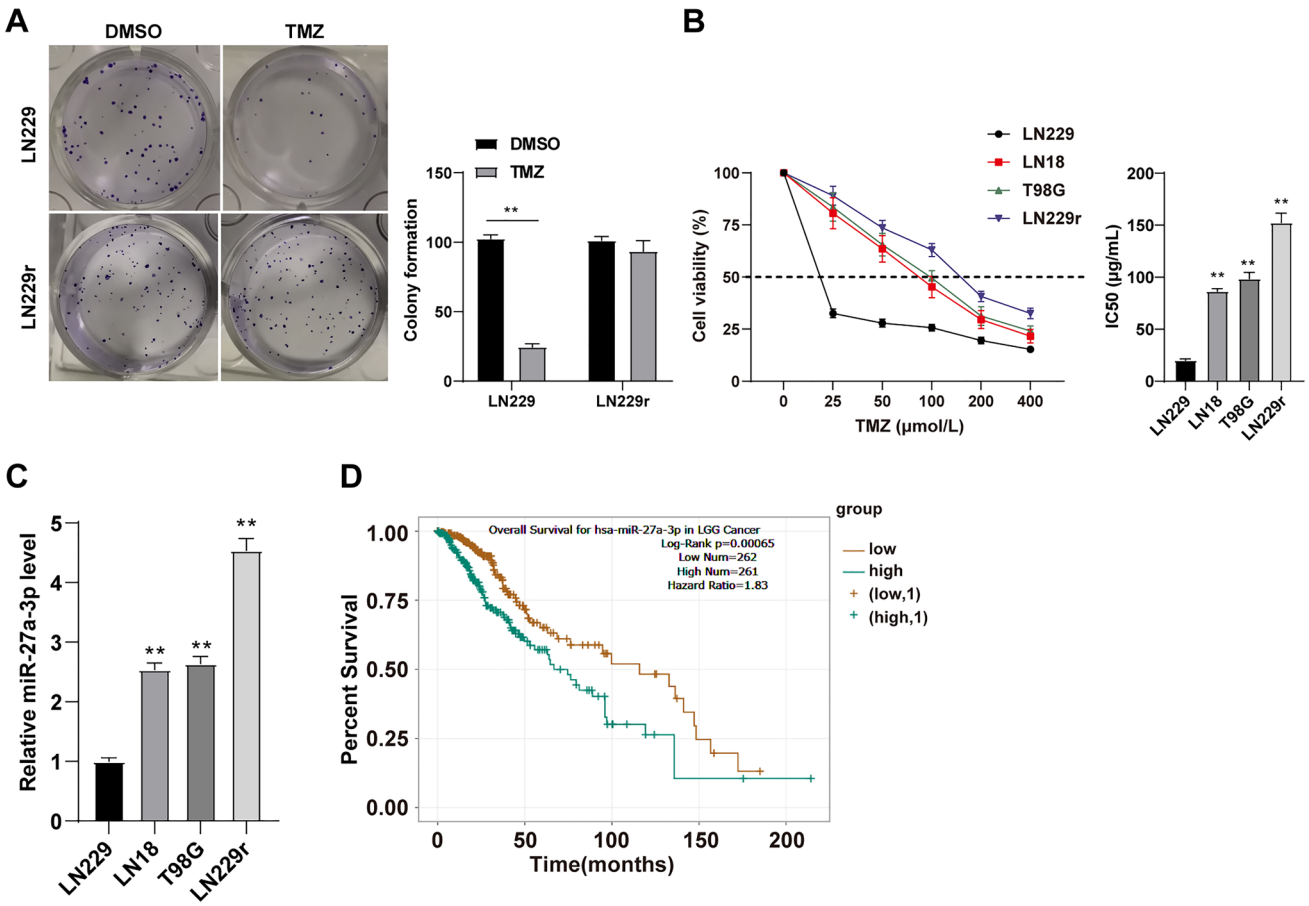

Fig. 1 miR-27a-3p was highly expressed in TMZ-resistant GBM cells. (**A**) LN229 cells were induced into TMZ-resistant strain step by step and verified by colony formation assay; (**B**) The drug resistance of GBM cells to TMZ was detected using MTT method; (**C**) The expression of miR-27a-3p was detected by RT-qPCR; (**D**) The relationship between the expression of miR-27a-3p and the survival of GBM patients was predicted using the database. Three independent tests were performed. Independent *t* test was used for comparison of data in panel **A** and one-way ANOVA was used for comparison of data in panel **B**/**C**. Tukey's multiple comparisons test was used for the post hoc test. $^{**}P < 0.01$

miR-27a-3p induced drug resistance of GBM to TMZ

To verify the role of miR-27a-3p in GBM resistance to TMZ, miR-27a-3p mimic was used to increase the expression of miR-27a-3p in LN229 cells and the expression of miR-27a-3p in LN229r (drug-resistant) cells was downregulated using miR-27a-3p inhibitor. RT-qPCR confirmed that the transfection was successful ($P < 0.01$, Fig. 2A). Subsequently, the sample was treated with different concentrations of TMZ. MTT assay elicited that miR-27a-3p overexpression significantly elevated IC50 of LN229 to TMZ, while inhibition of miR-27a-3p reduced IC50 of LN229r to TMZ ($P < 0.01$, Fig. 2B). In addition, 100 μmol/L TMZ-treated cells were taken for detection. After overexpression of miR-27a-3p, colony formation assay demonstrated that the proliferation of LN229 cells was increased and flow cytometry showed that the apoptosis rate was decreased; while downregulated miR-27a-3p decreased the proliferation of LN229r cells and increased the apoptosis rate ($P < 0.01$, Fig. 2C, D). In conclusion, overexpression of miR-27a-3p could increase the resistance of LN229 to TMZ, while inhibition of miR-27a-3p could reduce the resistance of LN229r to TMZ.

miR-27a-3p existed in EVs

Tumor EVs are important mediators of intercellular communication between tumor cells and other cells located in the microenvironment and farther away [7, 19, 20]. EVs carrying miRNAs in the tumor microenvironment affect drug resistance [3, 9, 21]. We speculated that the EVs might carry miR-27a-3p in the microenvironment of GBM cells to communicate with each other, thus affecting the drug resistance of GBM cells to TMZ. EVs were extracted from LN18 cells and observed in a typical cup with a size of about 20–500 nm ($P < 0.01$, Fig. 3A). NTA elicited that the average particle size of EVs was 84.78 ± 6.5 nm (Fig. 3B). WB demonstrated that there were CD63 and CD9 expressions but no calnexin expression in EVs (Fig. 3C). miR-27a-3p expression in EVs was detected by RT-qPCR and it was shown that miR-27a-3p expression in EVs was upregulated and the expression was not affected by RNase treatment, indicating that miR-27a-3p was encapsulated in EVs ($P < 0.01$, Fig. 3D). In conclusion, miR-27a-3p existed in EVs.

EVs shuttled miR-27a-3p promoted drug resistance of GBM to TMZ

To verify that miR-27a-3p shuttled by EVs induced the drug resistance of GBM to TMZ, EVs were labeled with Dil fluorescence staining and it was found that EVs could be internalized by LN229r (Fig. 4A), and RT-qPCR elicited that EVs treatment could upregulate miR-27a-3p expression in LN229r ($P < 0.01$, Fig. 4B). In addition, miR-27a-3p expression in LN18 was downregulated by miR-27a-3p inhibitor ($P < 0.01$, Fig. 4C). After transfection, EVs were extracted and the results showed that miR-27a-3p expression in EVs was also downregulated ($P < 0.01$, Fig. 4C), and the expression of miR-27a-3p in LN229r was also downregulated ($P < 0.01$, Fig. 4B). LN229r was treated with different concentrations of TMZ and the results showed that the IC50 of LN229r to TMZ was increased significantly after EVs treatment, while the IC50 was decreased after the EVs-inhibitor treatment ($P < 0.01$, Fig. 4D). In addition, 100 μmol/L TMZ-treated cells were used for detection. EVs treatment could increase the proliferation of LN229r cells and decrease apoptosis, while EVs treatment with downregulated miR-27a-3p showed the opposite trend ($P < 0.01$, Fig. 4E, F). In brief, LN18-derived EVs could be internalized by LN229r, release miR-27a-3p into LN229r, upregulate miR-27a-3p expression and increase the resistance of LN229r to TMZ.

miR-27a-3p targeted BTG2

To further investigate the downstream mechanism of the miR-27a-3p, target genes of miR-27a-3p were predicted using TargetScan database, among which BTG2 was downregulated in GBM [13]. According to the obtained binding sites (Fig. 5A), dual-luciferase assay was designed. The fluorescence intensity of BTG2 wild-type plasmid (WT) and miR-27a-3p mimic co-transfected group was lower than that of BTG2 mutant plasmid (MUT) and miR-27a-3p mimic co-transfected group, which confirmed that the targeted binding between miR-27a-3p and BTG2 ($P < 0.01$, Fig. 5B). In addition, intervention of miR-27a-3p expression could affect the expression of BTG2 ($P < 0.01$, Fig. 5C). EVs treatment could downregulate BTG2 expression in LN229r and BTG2 expression was partially upregulated after EVs-inhibitor treatment ($P < 0.01$, Fig. 5D). The results above indicated that LN18-derived EVs carried miR-27a-3p into LN229 cells and targeted BTG2.

Overexpression of BTG2 inhibited the effect of EVs on promoting TMZ resistance in GBM

To verify the role of BTG2 in TMZ resistance of GBM, the expression of BTG2 in LN229r cells of the EVs group was upregulated by pcDNA-BTG2 ($P < 0.01$, Fig. 6A). The sample was treated with different concentrations of TMZ. MTT assay, colony formation assay, and flow cytometry elicited that compared with the control group, IC50 value was decreased, proliferation was decreased, and apoptosis rate was increased in the BTG2 overexpression group ($P < 0.01$, Fig. 6B, D), suggesting that BTG2 overexpression reduced the resistance of LN229r cells to TMZ. In brief, overexpression of BTG2 inhibited the promoting effect of EVs on TMZ resistance in GBM.

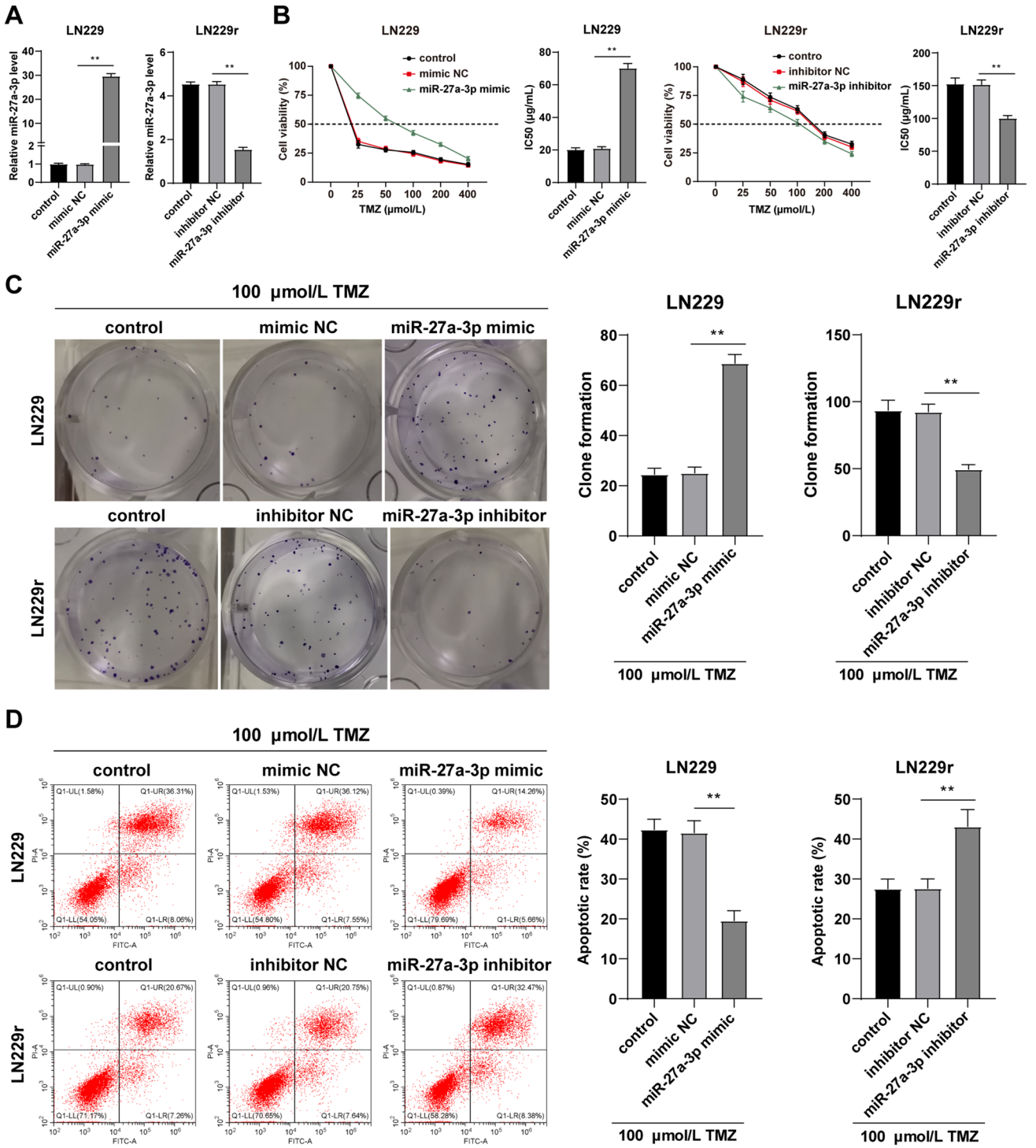

Fig. 2 miR-27a-3p induced drug resistance of GBM to TMZ. miR-27a-3p mimic was transfected into LN229 cells, and the transfected mimic NC was used as control. miR-27a-3p inhibitor was used to infect LN229r, and inhibitor NC was used as control. Untreated LN229 or LN229r were used as the control group. (**A**) The expression of miR-27a-3p was detected using RT-qPCR. The drug resistance of cells was detected using (**B**) MTT method, (**C**) colony formation assay, and (**D**) flow cytometry. Three independent tests were performed and the data were expressed as mean ± standard deviation. One-way ANOVA was used for comparisons of data in panels **A/B/C/D**. Tukey's multiple comparisons test was used for the post hoc test. $^{**}P < 0.01$

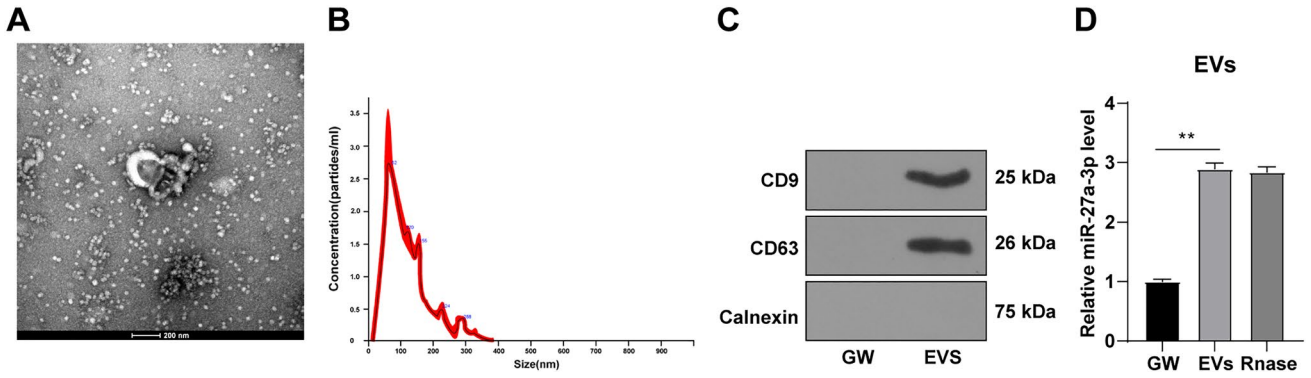

Fig. 3 miR-27a-3p existed in EVs. (**A**) The morphology of EVs secreted by LN18 was observed using TEM; (**B**) The concentration and particle size of EVs were measured using NTA; (**C**) WB was used to detect the expressions of CD9, CD63, and calnexin on the surface of LN18 derived EVs; (**D**) The expression of miR-27a-3p in EVs was detected by RT-qPCR. Three independent tests were performed and the data were expressed as mean ± standard deviation. One-way ANOVA was used for comparison of data in panel **D**. Tukey's multiple comparisons test was used for the post hoc test. $^{**}P < 0.01$

EVs carrying miR-27a-3p induced TMZ-resistance in nude mice with xenograft tumor

The xenograft tumor nude mouse model was established by injection of LN229r and the mice were treated with EVs and 100 μmol/L TMZ. After EVs treatment, the tumor volume and weight were significantly increased, and the positive rate of Ki67 was increased ($P < 0.05$, Fig. 7A–C). In addition, after EV treatment, miR-27a-3p was upregulated, while BTG2 was downregulated ($P < 0.01$, Fig. 7D, E). The results above indicated that EVs mediated the miR-27a-3p/BTG2 axis to promote the growth of xenograft tumors in nude mice.

Discussion

GBM is the most prevalent primary intracranial tumor, which represents about 81% of the malignant tumors of the brain [2]. Although there have been advances in clinical regimens and surgical techniques, high-grade GMB treatment remains challenging and the treatment success rate and overall survival rate remain very low [22]. Shreds of evidence have shown that EVs have pivotal roles in regulating drug resistance in GBM [23]. This study found that EVs carrying miR-27a-3p targeted BTG2, thus promoting TMZ-resistance of GBM.

miR-27a-3p is highly expressed and identified as an oncogene in a variety of cancers, including cervical cancer and colorectal cancer [24, 25]. Our results demonstrated that miR-27a-3p was upregulated in TMZ-resistant cells and the prognosis of GBM patients with high miR-27a-3p expression was poor. Consistently, miR-27a-3p is upregulated in GBM tissues [26]. miR-27a-3p can be used to be a potential biomarker for the prognosis of GBM [27]. To confirm the action of miR-27a-3p in TMZ resistance of GBM, miR-27a-3p in LN229 cells was overexpressed using miR-27a-3p mimic and miR-27a-3p in LN229r cells was inhibited using miR-27a-3p inhibitor and then cells were treated with different concentrations of TMZ. IC50 was conventionally used to quantify drug resistance and sensitivity [28]. Our results showed that miR-27a-3p overexpression increased the IC50 and proliferation of LN229 cells to TMZ and decreased apoptosis rate, while miR-27a-3p inhibition decreased the IC50 and proliferation of LN229r cells and increased apoptosis rate. It is consistent that miR-27a-3p induces TMZ resistance in GBM [18]. In conclusion, miR-27a-3p overexpression increased the resistance of LN229 to TMZ, while miR-27a-3p inhibition reduced the resistance of LN229r to TMZ.

EVs are the important mediators for the communications between tumors and normal cells [7]. Maisano et al. have shown that some tumors change the movement, angiogenesis, and immune-related functions of other cells through EV transmission [20]. Kara-Terki et al. have shown that tumor cells can transfer miRNA through EVs to affect the phenotype and motor behaviors of normal cells [7]. Zeng A et al. have shown that drug-resistant donor cells can transfer miRNA through EVs to affect the drug resistance of recipient cells [21]. EVs transfer miRNAs to regulate TMZ-resistance in GBM [9]. Therefore, we speculated that EVs transferred miR-27a-3p in the microenvironment of GBM cells and allowed intercellular communication between tumor cells and normal cells, thus influencing the TMZ-resistance of GBM. Our results identified EVs through EV positive markers CD63, CD9, and negative markers endoplasmic reticulum specific molecule calnexin [29, 30] and elicited that miR-27a-3p expression in EVs was upregulated and the expression wasn't changed by RNase treatment. In conclusion, miR-27a-3p was encapsulated in EVs. EVs transmit

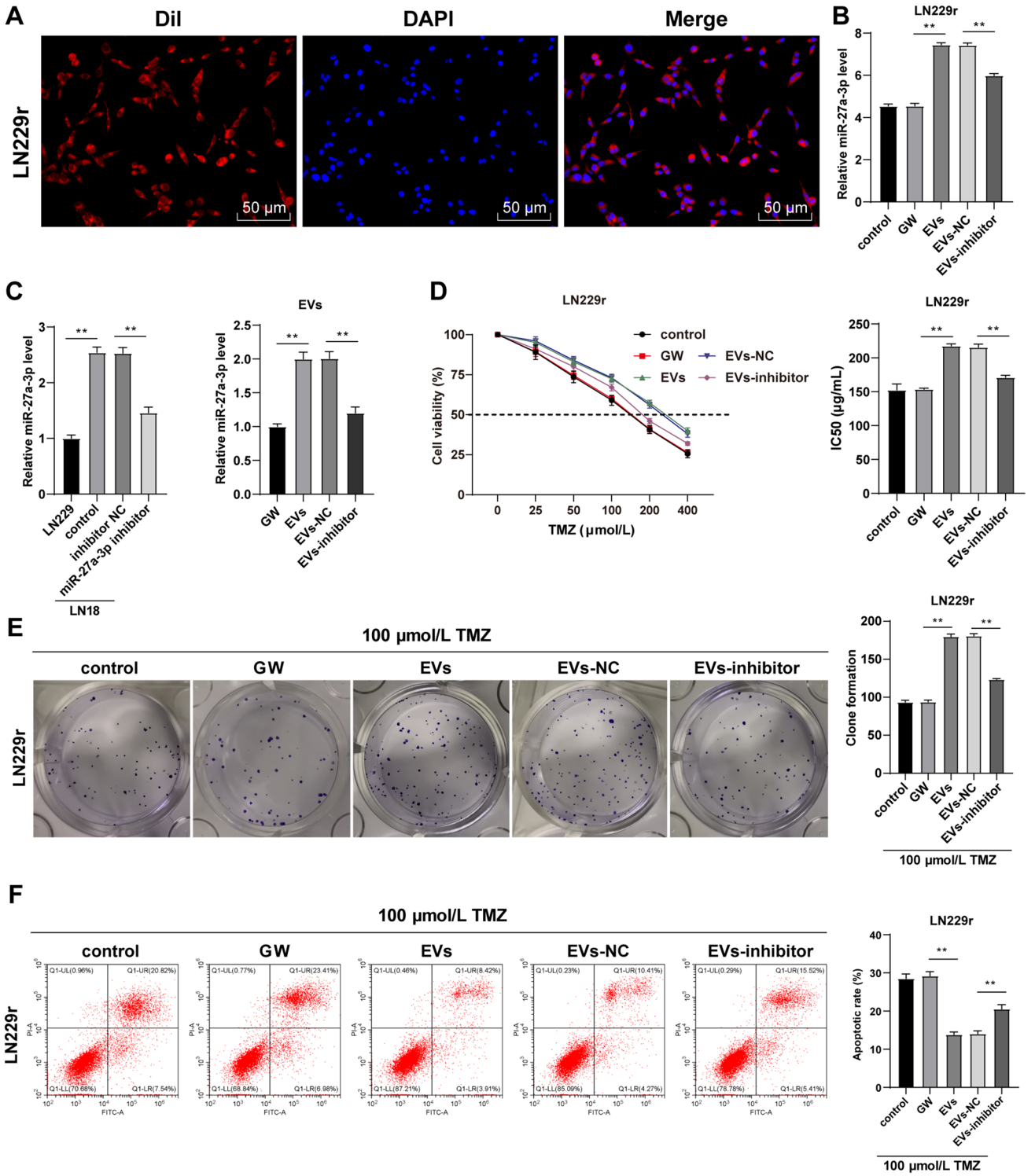

Fig. 4 EVs carrying miR-27a-3p induced drug resistance of GBM to TMZ. (**A**) The internalization of Dil-labeled EVs by LN229r was observed under a fluorescence microscope; EVs or EVs with down-regulated miR-27a-3p were extracted to act on LN229r; (**B**, **C**) miR-27a-3p expressions in LN229r, LN18, and EVs were detected by RT-qPCR. The drug resistance of cells was detected using (**D**) MTT method, (**E**) colony formation assay, and (**F**) flow cytometry. Three independent tests were performed and the data were expressed as mean ± standard deviation. One-way ANOVA was used for comparisons of data in panels B/C/D/E/F. Tukey's multiple comparisons test was used for the post hoc test. $^{**}P < 0.01$. GW group (co-culture of GW4869-treated LN18 cell extract and LN229r cells), EVs group (co-culture of LN18-derived EVs and LN229r cells), EVs-NC group (co-culture of LN18-derived EVs transfected with inhibitor NC and LN229r cells), EVs-inhibitor group (co-culture of LN18-derived EVs transfected with miR-27a-3p inhibitor and LN229r cells), control group (co-culture of equal volume PBS and LN229r cells)

A

	Predicted consequential pairing of target region (top) and miRNA (bottom)	Site type	Context++ score	Context++ score percentile	Weighted context++ score	Conserved branch length	P_{CT}
Position 361-368 of BTG2 3' UTR	5' ...CAAGCAAGGUUAGCAACUGUGAA...	8mer	-0.34	98	-0.34	4.535	0.74
hsa-miR-27a-3p	3' CGCCUUGAAUCGGUGACACUU						

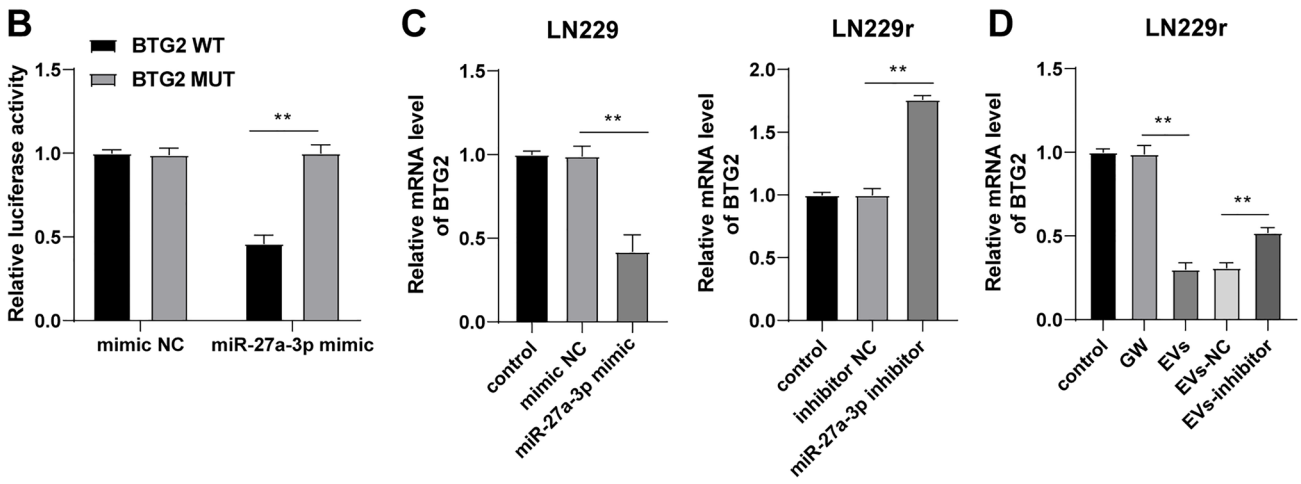

Fig. 5 miR-27a-3p targeted BTG2. (**A**) The binding sites of miR-27a-3p and BTG2 were predicted using TargetScan database; (**B**) The binding relationship between miR-27a-3p and BTG2 was verified by dual-luciferase assay; (**C**, **D**) The expression of BTG2 in LN229 and LN229r cells were detected by RT-qPCR. Three independent tests were performed and the data were expressed as mean ± standard deviation. Independent *t* test was used for comparison of data in panel B and one-way ANOVA was used for comparison of data in panels **C**/**D**. Tukey's multiple comparisons test was used for the post hoc test. $^{**}P < 0.01$

drug resistance in cancers [31]. Our results showed that EVs could be internalized by LN229r cells, and EVs treatment upregulated miR-27a-3p expression in LN229r cells. miR-27a-3p in LN18 cells was inhibited using miR-27a-3p inhibitor. The results showed that miR-27a-3p expression in EVs was downregulated after the transfection. The IC50 of LN229r cells to TMZ and LN229r cell proliferation was increased and the apoptosis was decreased after EVs treatment, while the EVs-inhibitor treatment showed the opposite trend. However, there is no report at present on EVs carrying miR-27a-3p promoting TMZ-resistance in GBM. Our study found that LN18-derived EVs could be internalized by LN229r cells, then release miR-27a-3p into LN229r cells, upregulate miR-27a-3p expression, and increase the TMZ-resistance of LN229r cells.

To study the downstream mechanism of miR-27a-3p, we used TargetScan database to predict the downstream target genes of miR-27a-3p. Then BTG2 was obtained. BTG2 is an important anti-proliferation gene and its reduction is closely related to a poor prognosis of GBM patients [12]. Dual-luciferase assay confirmed the targeted binding relationship between miR-27a-3p and BTG2. Our results demonstrated that EV treatment downregulated BTG2 expression in LN229, and BTG2 expression was partially upregulated after treatment of EVs-inhibitor. Consistently, BTG2 was downregulated in GBM tissues [13]. In conclusion, LN18 derived EVs carried miR-27a-3p into LN229 cells and targeted BTG2. Moreover, we overexpressed BTG2 in LN229r cells of THE EVs group. Our results demonstrated that after BTG2 overexpression, IC50 value was decreased, proliferation was decreased and apoptosis rate was increased. Similarly, BTG-2 overexpression reversed the inhibitory action of miR-134-5p on glioma cell proliferation and migration [32]. In brief, BTG2 overexpression inhibited the effect of EVs on promoting TMZ resistance in GBM.

In summary, this study supported that tumor cell-derived EVs encapsulated miR-27a-3p and delivered it in the tumor microenvironment. After being internalized by other tumor cells, EVs released miR-27a-3p to increase miR-27a-3p expression in cells, and targeted BTG2, thus inducing the TMZ-resistance of GBM. However, the roles of other miRNAs in EVs and other downstream target genes of miR-27a-3p have not been explored, and the downstream passage of BTG2 is also unknown. Further work is needed to verify the role of other miRNAs in EVs and other downstream target genes of miR-27a-3p.

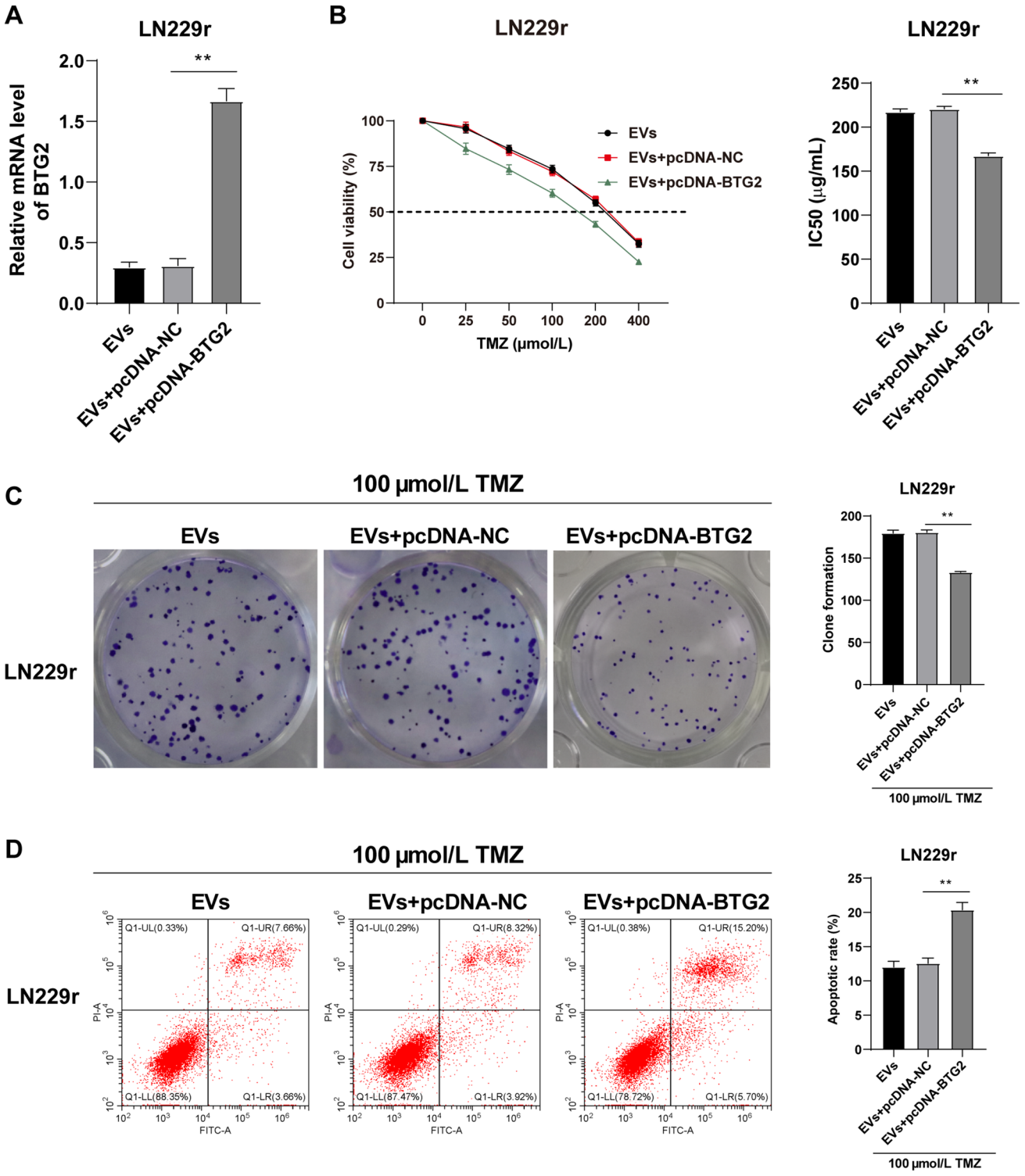

Fig. 6 Overexpression of BTG2 inhibited the effect of EVs on promoting TMZ resistance in GBM. (**A**) Interference efficiency of pcDNA-BTG2 was detected by RT-qPCR; The drug resistance of cells was detected using (**B**) MTT method, (**C**) colony formation assay, and (**D**) flow cytometry. Three cell tests were performed and the data were expressed as mean ± standard deviation. One-way ANOVA was used for comparisons of data. Tukey's multiple comparisons test was used for the post hoc test. $^{**}P < 0.01$. EVs group (EVs-treated LN229r cells), EVs + pcDNA-BTG2 group (EVs-treated LN229r cells were transfected with pcDNA-BTG2), EVs + pcDNA-NC group (EVs-treated LN229r cells were transfected with pcDNA-NC)

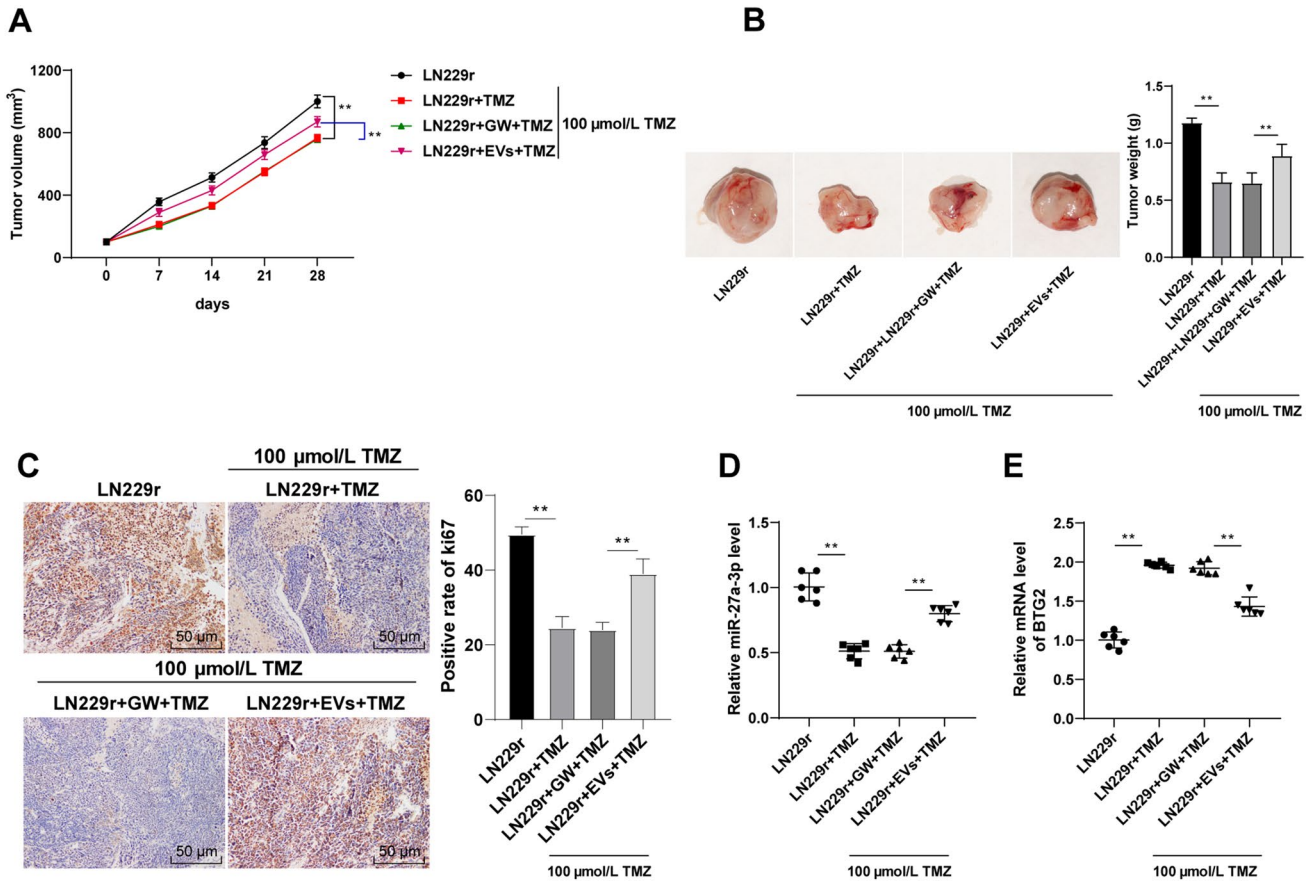

Fig. 7 EVs carrying miR-27a-3p induced TMZ-resistance in nude mice with xenograft tumor. LN229r cells were injected into mice to induce subcutaneous tumorigenesis, and the mouse was treated with EVs. The equal GW4869-treated LN18-conditioned medium was used as the control group. The mouse was injected with 100 μmol/L TMZ. (**A**) The tumor volume of mice on different days; (**B**) Comparison of tumor volume and weight of mice in each group; (**C**) The positive rate of Ki67 was detected by immunohistochemistry; (**D**, **E**) The expressions of miR-27a-3p and BTG2 were analyzed by RT-qPCR; $N=6$. The data in panels **A/B/C** were expressed as mean ± standard deviation. One-way ANOVA was used for comparisons of data. Tukey's multiple comparisons test was used for the post hoc test. $^{*}P<0.05$, $^{**}P<0.01$

Funding Not applicable.

Declarations

Conflict of interest The authors declare no conflict of interest.

References

1. Chen R, Smith-Cohn M, Cohen AL, Colman H (2017) Glioma subclassifications and their clinical significance. Neurotherapeutics 14(2):284–297. https://doi.org/10.1007/s13311-017-0519-x
2. Ostrom QT, Bauchet L, Davis FG, Deltour I, Fisher JL, Langer CE, Pekmezci M, Schwartzbaum JA, Turner MC, Walsh KM, Wrensch MR, Barnholtz-Sloan JS (2014) The epidemiology of glioma in adults: a "state of the science" review. Neuro Oncol 16(7):896–913. https://doi.org/10.1093/neuonc/nou087
3. Kosgodage US, Uysal-Onganer P, MacLatchy A, Kraev I, Chatterton NP, Nicholas AP, Inal JM, Lange S (2018) Peptidylarginine deiminases post-translationally deiminate prohibitin and modulate extracellular vesicle release and MicroRNAs in glioblastoma multiforme. Int J Mol Sci. https://doi.org/10.3390/ijms20010103
4. Mostafa H, Pala A, Hogel J, Hlavac M, Dietrich E, Westhoff MA, Nonnenmacher L, Burster T, Georgieff M, Wirtz CR, Schneider EM (2016) Immune phenotypes predict survival in patients with glioblastoma multiforme. J Hematol Oncol 9(1):77. https://doi.org/10.1186/s13045-016-0272-3
5. Stupp R, Mason WP, van den Bent MJ, Weller M, Fisher B, Taphoorn MJ, Belanger K, Brandes AA, Marosi C, Bogdahn U, Curschmann J, Janzer RC, Ludwin SK, Gorlia T, Allgeier A, Lacombe D, Cairncross JG, Eisenhauer E, Mirimanoff RO, European Organisation for R, Treatment of Cancer Brain T, Radiotherapy G, National Cancer Institute of Canada Clinical Trials G (2005) Radiotherapy plus concomitant and adjuvant temozolomide for glioblastoma. N Engl J Med 352(10):987–996. https://doi.org/10.1056/NEJMoa043330
6. Gusyatiner O, Hegi ME (2018) Glioma epigenetics: from subclassification to novel treatment options. Semin Cancer Biol 51:50–58. https://doi.org/10.1016/j.semcancer.2017.11.010
7. Kara-Terki L, Treps L, Blanquart C, Fradin D (2020) Critical roles of tumor extracellular vesicles in the microenvironment

of thoracic cancers. Int J Mol Sci. https://doi.org/10.3390/ijms21176024
8. Zhang C, Yang X, Fu C, Liu X (2018) Combination with TMZ and miR-505 inhibits the development of glioblastoma by regulating the WNT7B/Wnt/beta-catenin signaling pathway. Gene 672:172–179. https://doi.org/10.1016/j.gene.2018.06.030
9. Yin J, Zeng A, Zhang Z, Shi Z, Yan W, You Y (2019) Exosomal transfer of miR-1238 contributes to temozolomide-resistance in glioblastoma. EBioMedicine 42:238–251. https://doi.org/10.1016/j.ebiom.2019.03.016
10. Li Y, Liu Y, Ren J, Deng S, Yi G, Guo M, Shu S, Zhao L, Peng Y, Qi S (2018) miR-1268a regulates ABCC1 expression to mediate temozolomide resistance in glioblastoma. J Neurooncol 138(3):499–508. https://doi.org/10.1007/s11060-018-2835-3
11. Zhang Z, Xu J, Chen Z, Wang H, Xue H, Yang C, Guo Q, Qi Y, Guo X, Qian M, Wang S, Qiu W, Gao X, Zhao R, Guo X, Li G (2020) Transfer of MicroRNA via macrophage-derived extracellular vesicles promotes proneural-to-mesenchymal transition in glioma stem cells. Cancer Immunol Res 8(7):966–981. https://doi.org/10.1158/2326-6066.CIR-19-0759
12. Yuniati L, Scheijen B, van der Meer LT, van Leeuwen FN (2019) Tumor suppressors BTG1 and BTG2: beyond growth control. J Cell Physiol 234(5):5379–5389. https://doi.org/10.1002/jcp.27407
13. Li WQ, Yu HY, Zhong NZ, Hou LJ, Li YM, He J, Liu HM, Xia CY, Lu YC (2015) miR27a suppresses the clonogenic growth and migration of human glioblastoma multiforme cells by targeting BTG2. Int J Oncol 46(4):1601–1608. https://doi.org/10.3892/ijo.2015.2843
14. Lee SY (2016) Temozolomide resistance in glioblastoma multiforme. Genes Dis 3(3):198–210. https://doi.org/10.1016/j.gendis.2016.04.007
15. Ying H, Lin F, Ding R, Wang W, Hong W (2020) Extracellular vesicles carrying miR-193a derived from mesenchymal stem cells impede cell proliferation, migration and invasion of colon cancer by downregulating FAK. Exp Cell Res 394(2):112144. https://doi.org/10.1016/j.yexcr.2020.112144
16. Agarwal V, Bell GW, Nam JW, Bartel DP (2015) Predicting effective microRNA target sites in mammalian mRNAs. Elife. https://doi.org/10.7554/eLife.05005
17. Livak KJ, Schmittgen TD (2001) Analysis of relative gene expression data using real-time quantitative PCR and the 2(-Delta Delta C(T)) Method. Methods 25(4):402–408. https://doi.org/10.1006/meth.2001.1262
18. Li S, Li W, Chen G, Huang J, Li W (2020) MiRNA-27a-3p induces temozolomide resistance in glioma by inhibiting NF1 level. Am J Transl Res 12(8):4749–4756
19. Zhang J, Xiao X, Zhang X, Hua W (2020) Tumor microenvironment characterization in glioblastoma identifies prognostic and immunotherapeutically relevant gene signatures. J Mol Neurosci 70(5):738–750. https://doi.org/10.1007/s12031-020-01484-0
20. Maisano D, Mimmi S, Russo R, Fioravanti A, Fiume G, Vecchio E, Nistico N, Quinto I, Iaccino E (2020) Uncovering the exosomes diversity: a window of opportunity for tumor progression monitoring. Pharmaceuticals (Basel). https://doi.org/10.3390/ph13080180
21. Zeng A, Wei Z, Yan W, Yin J, Huang X, Zhou X, Li R, Shen F, Wu W, Wang X, You Y (2018) Exosomal transfer of miR-151a enhances chemosensitivity to temozolomide in drug-resistant glioblastoma. Cancer Lett 436:10–21. https://doi.org/10.1016/j.canlet.2018.08.004
22. Malta TM, de Souza CF, Sabedot TS, Silva TC, Mosella MS, Kalkanis SN, Snyder J, Castro AVB, Noushmehr H (2018) Glioma CpG island methylator phenotype (G-CIMP): biological and clinical implications. Neuro Oncol 20(5):608–620. https://doi.org/10.1093/neuonc/nox183
23. Simon T, Jackson E, Giamas G (2020) Breaking through the glioblastoma micro-environment via extracellular vesicles. Oncogene 39(23):4477–4490. https://doi.org/10.1038/s41388-020-1308-2
24. Su C, Huang DP, Liu JW, Liu WY, Cao YO (2019) miR-27a-3p regulates proliferation and apoptosis of colon cancer cells by potentially targeting BTG1. Oncol Lett 18(3):2825–2834. https://doi.org/10.3892/ol.2019.10629
25. Ben W, Zhang G, Huang Y, Sun Y (2020) MiR-27a-3p regulated the aggressive phenotypes of cervical cancer by targeting FBXW7. Cancer Manag Res 12:2925–2935. https://doi.org/10.2147/CMAR.S234897
26. Xu W, Liu M, Peng X, Zhou P, Zhou J, Xu K, Xu H, Jiang S (2013) miR-24-3p and miR-27a-3p promote cell proliferation in glioma cells via cooperative regulation of MXI1. Int J Oncol 42(2):757–766. https://doi.org/10.3892/ijo.2012.1742
27. Salmani T, Ghaderian SMH, Hajiesmaeili M, Rezaeimirghaed O, Hoseini MS, Rakhshan A, Nasiri MJ, Ghaedi H, Akbarzadeh R (2020) Hsa-miR-27a-3p and epidermal growth factor receptor expression analysis in glioblastoma FFPE samples. Asia Pac J Clin Oncol. https://doi.org/10.1111/ajco.13399
28. Hafner M, Niepel M, Chung M, Sorger PK (2016) Growth rate inhibition metrics correct for confounders in measuring sensitivity to cancer drugs. Nat Methods 13(6):521–527. https://doi.org/10.1038/nmeth.3853
29. Torres Crigna A, Fricke F, Nitschke K, Worst T, Erb U, Karremann M, Buschmann D, Elvers-Hornung S, Tucher C, Schiller M, Hausser I, Gebert J, Bieback K (2021) Inter-laboratory comparison of extracellular vesicle isolation based on ultracentrifugation. Transfus Med Hemother 48(1):48–59. https://doi.org/10.1159/000508712
30. Jiao R, Sun S, Gao X, Cui R, Cao G, Wei H, Wang S, Zhang Z, Bai H (2020) A polyethylene glycol-based method for enrichment of extracellular vesicles from culture supernatant of human ovarian cancer cell line A2780 and body fluids of high-grade serous carcinoma patients. Cancer Manag Res 12:6291–6301. https://doi.org/10.2147/CMAR.S228288
31. O'Neill CP, Gilligan KE, Dwyer RM (2019) Role of extracellular vesicles (EVs) in cell stress response and resistance to cancer therapy. Cancers (Basel). https://doi.org/10.3390/cancers11020136
32. Tong H, Zhao K, Wang J, Xu H, Xiao J (2020) CircZNF609/miR-134-5p/BTG-2 axis regulates proliferation and migration of glioma cell. J Pharm Pharmacol 72(1):68–75. https://doi.org/10.1111/jphp.13188